

STABILIZED FINITE ELEMENT SIMULATION OF DOUBLE DIFFUSIVE NATURAL CONVECTION

March, R.^a, Coutinho, A.L.G.A.^a and Elias, R.N.^b

^a NACAD-High Performance Computing Laboratory, COPPE/Federal University of Rio de Janeiro, Rio de Janeiro, Brazil, <http://www.nacad.ufrj.br>

^b The Federal Rural University of Rio de Janeiro, Rio de Janeiro, Brazil, <http://www.ufrj.br>

Keywords: Stabilized Finite Element Methods, Double-diffusive Convection, Computational Fluid Dynamics

Abstract. Double-diffusion is a type of flow driven mainly by buoyancy forces, induced by the gradients of thermal energy and concentration of a chemical component. The understanding of this kind of phenomena is essential for many scientific and engineering applications. Computational fluid dynamics can be used to aid the understanding of the behavior of the temperature and concentration fields in this kind of phenomena. A stabilized finite element formulation is described and used to simulate double-diffusive process in a rectangular cavity, for several values of buoyancy rate, Lewis and Rayleigh number and it shows to be adequate for this kind of multiphysics problems.

1 INTRODUCTION

Double-diffusion is a type of flow driven mainly by buoyancy forces, induced by the gradients of thermal energy and concentration of a chemical component. This type of phenomena can be found in many situations in nature and engineering. In oceanography, the sea can be considered a multicomponent domain, with the presence of salts, and the heating of the surface starts a double-diffusive process which drives the water masses and dictates the circulation. In engineering, double-diffusion has applications the design of solar power collectors, oil recovery and food processing, to name just a few. Therefore, it is of extreme importance the detailed understanding of the physics of this phenomena, and the knowledge of which parameters affects the flow behavior.

Computational fluid dynamics can be used to simulate double-diffusive processes aiding the scientific and engineering community in the understanding of this complex phenomenon. There has been many scientific works devoted in the use of CFD in this field. [Sezai and Mohamad \(2000\)](#) used the finite volume method to perform a three-dimensional simulation of double-diffusion in a cubic cavity. [Kamakura and Ozoe \(2002\)](#) simulated double-diffusive convection in a salt stratified system, at high Rayleigh numbers. [Sripada and Angirasa \(2001\)](#) performed two-dimensional simulations of double-diffusion in upward facing horizontal surfaces. [Chamkha and Al-Naser \(2002\)](#) evaluated the effect of a magnetic field in double-diffusive natural convection. [Yahiaoui et al. \(2007\)](#) analysed this process in a vertical annular cavity. [Kim and Rani \(2009\)](#) analysed Dufour and Soret effects in double-diffusion. [Cheng \(2009\)](#) investigates the heat and mass transfer over a vertical cone in a fluid saturated porous media

In the past of computational flow dynamics field, the finite element method was not so popular in comparison to the finite volumes or finite differences method. This was due to the incapability of the standard Galerkin formulation to deal properly with predominantly advective problems. In this context, the stabilized formulations arised to overcome this limitation. Therefore, stabilized formulations may be a good candidate to be tested in the solution of complex multiphysics problems. In this work, we will analyze the influence of some nondimensional groups in a double-diffusive phenomena using a stabilized finite element method.

2 GEOMETRY, BOUNDARY CONDITIONS AND GOVERNING EQUATIONS

The system of equations considered is

$$\begin{aligned} \nabla \cdot \mathbf{u} &= 0 \\ \rho \frac{\partial \mathbf{u}}{\partial t} + \rho (\mathbf{u} \cdot \nabla) \mathbf{u} &= -\nabla p + \mu \nabla^2 \mathbf{u} + \rho^* \mathbf{g} \\ \frac{\partial T}{\partial t} + \mathbf{u} \cdot \nabla T &= \alpha \nabla^2 T \\ \frac{\partial C}{\partial t} + \mathbf{u} \cdot \nabla C &= D \nabla^2 C \end{aligned} \quad (1)$$

,which are essentially the Navier-Stokes equations, plus the advection-diffusion of thermal energy and the concentration of a component, assuming a binary mixture. All the coefficients are assumed constant, except for the density, whose variation is considered to be important only in the body force term, to take account for the buoyancy effect. This is expressed as a first-order variation of the density with the temperature and concentration, that is

$$\rho^* = \rho [1 - \beta_T (T - T_{REF}) + \beta_C (C - C_{REF})] \quad (2)$$

This is known as the *Boussinesq Approximation*. This is generally assumed to be reasonable for short variations in the temperature and in the concentration, which is the case considered here. The exchanged signal in the concentration term is to impose an opposing concentration gradient.

The solution of double-diffusive and natural convection problems is influenced by the values of the following nondimensional parameters:

- $Pr = \frac{\nu}{\alpha}$ - The *Prandtl* number is the ratio of viscous diffusivity and the thermal diffusivity parameters.
- $Le = \frac{\alpha}{D}$ - The *Lewis* number is the ratio of thermal diffusivity and the mass diffusivity parameters.
- $Ra = \frac{g\alpha_T(T_L - T_R)b^3}{\nu\alpha}$ - The *thermal Rayleigh* number can be viewed as the as a parameter to measure whether the heat transfer occurs mainly by convection or by conduction
- $N = \frac{\alpha_C(C_L - C_R)}{\alpha_T(T_L - T_R)}$ - The *buoyancy ratio* measures if the buoyancy forces are mainly affected by thermal energy or by the concentration gradients

The fluid is initially assumed to be motionless. The motion will be started and driven by buoyancy forces, as density varies from a point to another according to the values of the temperature and the concentration. The geometry is a simple rectangular cavity, with aspect ratio $A = \frac{h}{b} = 2$, and the boundary conditions are shown in figure 1:

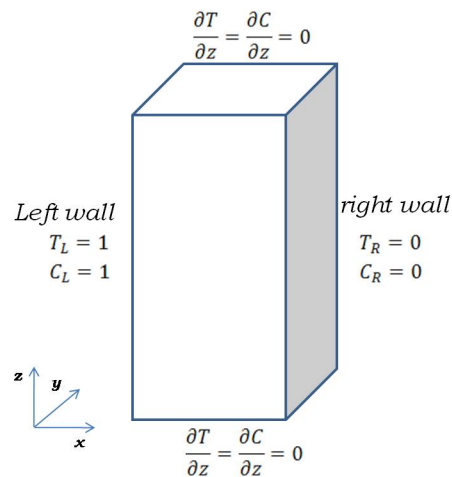


Figure 1: Geometry and Boundary Conditions

No-slip conditions are set for the walls, the initial temperature and concentration fields are set to be $T_0 = 0$ and $C_0 = 0$.

3 NUMERICAL PROCEDURE

A stabilized finite element formulation is used in the spatial discretization of the flow and transport (temperature and concentration) equations. It is well known that the standard Galerkin Finite Element Method (GFEM), which consists of weighting the equation and then integrating in the domain, gives oscillatory non-physical results as the Reynolds number (or simply the Peclét number, for the transport equations) is increased. Therefore, stabilized formulations were developed to overcome this limitation of the method [Tezduyar \(1992\)](#). The formulation used here is called the *SUPG-Streamline Upwind Petrov-Galerkin*, developed in [Brooks and Hughes \(1982\)](#). Additional crosswind dissipation is added to the formulation to treat large gradients - jumps - in the values of the variables. This is usually called *shock capturing operator*, and the one used here was firstly presented in [Codina \(1993\)](#); and usually shows good accuracy, by not smearing too much the solution.

Time integration is done by a *Predictor-Multicorrector* strategy [Hughes \(2003\)](#). The flow and transport equations are advanced in time by iterating at each time step due to a predefined tolerance. In a timestep the initial discrete Navier-Stokes equations are solved until convergence is achieved for the given mesh. This involves solving a nonlinear system of equations - which is done by the *Inexact Newton's Method* [Elias et al. \(2006\)](#) - until convergence in the timestep. Then, the velocity field is used to evolve the temperature and concentration equations, which are also advanced iteratively in the timestep. A preconditioned *GMRES* solver is used in the solution of the linear systems.

3.1 Finite Element Formulation of the Navier-Stokes Equations

The finite element form of the Navier-Stokes equations is given by:

- Find $\mathbf{u}^h \in S_{\mathbf{u}}^h$ and $p^h \in S_p^h$ such that $\forall \mathbf{w}^h \in V_{\mathbf{u}}^h$ and $\forall q^h \in V_p^h$

$$\begin{aligned}
 & \int_{\Omega} \mathbf{w}^h \cdot \rho \left(\frac{\partial \mathbf{u}^h}{\partial t} + (\mathbf{u}^h \cdot \nabla) \mathbf{u}^h - \mathbf{f}^h \right) d\Omega - \int_{\Omega} (\nabla \cdot \mathbf{w}^h) p^h d\Omega + \\
 & \int_{\Omega} \epsilon(\mathbf{w}^h) : 2\mu \epsilon(\mathbf{u}^h) d\Omega + \int_{\Omega} q^h (\nabla \cdot \mathbf{u}^h) d\Omega + \\
 & \sum_{e=1}^{nel} \int_{\Omega^e} \frac{1}{\rho} [\tau_{SUPG} \rho (\mathbf{u}^h \cdot \nabla) \mathbf{w}^h + \tau_{PSPG} \nabla q^h] \cdot \\
 & \left[\rho \left(\frac{\partial \mathbf{u}^h}{\partial t} + (\mathbf{u}^h \cdot \nabla) \mathbf{u}^h \right) + \nabla p^h - \mu \nabla^2 \mathbf{u}^h - \rho \mathbf{f}^h \right] d\Omega^e + \\
 & \sum_{e=1}^{nel} \int_{\Omega^e} \tau_{LSIC} \nabla \cdot \mathbf{w}^h \rho \nabla \cdot \mathbf{u}^h d\Omega^e = \\
 & \int_{\partial\Omega} \mathbf{w}^h \cdot \mathbf{h}^h d\Gamma
 \end{aligned} \tag{3}$$

, where $S_{\mathbf{u}}^h, S_p^h, V_{\mathbf{u}}^h, V_p^h$ are convenient finite element interpolating spaces. The continuous domain is discretized into a finite set of elements - in the case here tetrahedra - and a function called *shape function* is associated with each element node (For more information, see [Hughes \(2003\)](#)). The trial and weight functions are then approximated by these functions, inside each element. This gives rise to a nonlinear set of temporal differential equations, which are solved by a predictor-multicorrector method. The terms preceded by a sum are additional stabilization

terms, designed to prevent oscillations but at the same time keeping the equations variationally consistent (one should note that they are usually proportional to the residua). The first is the *SUPG* stabilization, to prevent oscillations arising in standard Galerkin discretization of advective terms. The second is the *PSPG* stabilization Tezduyar (1992), to circumvent the *LBB-Stability problem* arising from using the same interpolation nodes and elements for the velocity and pressure degrees of freedom. The last is the *LSIC* stabilization Tezduyar (1992), for high Reynolds flows. Note that these terms are written as a summing due to the discontinuity of the stabilization parameters τ_{SUPG}, τ_{PSPG} and τ_{LSIC} . These parameters are calculated as follows:

$$\tau_{SUPG} = \tau_{PSPG} = \left[\left(\frac{2|\mathbf{u}^h|}{h} \right)^2 + 9 \left(\frac{4\nu}{h^2} \right)^2 \right]^{-\frac{1}{2}} \quad (4)$$

$$\tau_{LSIC} = \frac{|\mathbf{u}^h|h}{2} \quad (5)$$

where the element length h is calculated as the radius of the sphere which circumscribes the element. This definition has the only advantage of being simple, and it is well known that may not be suitable for stretched or high aspect ratio elements. One should avoid these elements in the mesh design step when using this definition.

It is important to remember that the coupling between these equation and the discrete temperature and concentration fields occurs in the body force term, written here as:

$$\mathbf{f}^h = \rho \mathbf{g}^h - \rho \mathbf{g}^h \beta_T (T^h - T_{REF}) + \rho \mathbf{g}^h \beta_C (C^h - C_{REF}) \quad (6)$$

3.2 Finite Element Discretization of the Temperature and Concentration Equations

The variational or weak form of the temperature and concentration equations are given by:

- Find $T^h \in S_T^h$ such that $\forall w^h \in V_T^h$

$$\begin{aligned} & \int_{\Omega} \left(w^h \frac{\partial T^h}{\partial t} + w^h \mathbf{u}^h \cdot \nabla T^h + \alpha \nabla w^h \cdot \nabla T^h \right) d\Omega \\ & + \sum_{e=1}^{nel} \int_{\Omega^e} \tau_{SUPG} \mathbf{u}^h \cdot \nabla w^h \left(\frac{\partial T^h}{\partial t} + \mathbf{u}^h \cdot \nabla T^h - \alpha \nabla w^h \cdot \nabla T^h \right) d\Omega \\ & + \sum_{e=1}^{nel} \int_{\Omega^e} \delta(T^h) \nabla w^h \cdot \nabla T^h d\Omega = \int_{\Omega} w^h h^h d\Omega \end{aligned}$$

- Find $C^h \in S_C^h$ such that $\forall w^h \in V_C^h$

$$\begin{aligned} & \int_{\Omega} \left(w^h \frac{\partial C^h}{\partial t} + w^h \mathbf{u}^h \cdot \nabla C^h + D \nabla w^h \cdot \nabla C^h \right) d\Omega \\ & + \sum_{e=1}^{nel} \int_{\Omega^e} \tau_{SUPG} \mathbf{u}^h \cdot \nabla w^h \left(\frac{\partial C^h}{\partial t} + \mathbf{u}^h \cdot \nabla C^h - D \nabla w^h \cdot \nabla C^h \right) d\Omega \\ & + \sum_{e=1}^{nel} \int_{\Omega^e} \delta(C^h) \nabla w^h \cdot \nabla C^h d\Omega = \int_{\Omega} w^h h^h d\Omega \end{aligned}$$

where again S_T^h and V_T^h are finite element interpolating spaces. The SUPG stabilization were already explained above, but a new nonlinear term is included in the transport equations, which is the shock capturing operator. Note that this term is similar to the diffusion term, but with the artificial diffusion coefficient, $\delta(T^h)$ and $\delta(C^h)$ respectively, being nonlinear. The coupling of these equations with the flow fields is seen in the advective terms.

4 VALIDATION OF THE METHOD

The method and the approaches described above are validated against results reported in [Chen et al. \(2010\)](#). The authors simulate a rectangular bidimensional cavity with boundary values of $T_L = C_L = 0.5$ and $T_R = C_R = -0.5$, with $Pr = 1, Le = 2, Ra = 10^5$ and $N = 0.8$. The figures below show a comparison between its results and the results obtained using the finite element formulation presented above. It can be seen that results are highly similar to the results of Chen et al., which validates the method for this kind of problems.

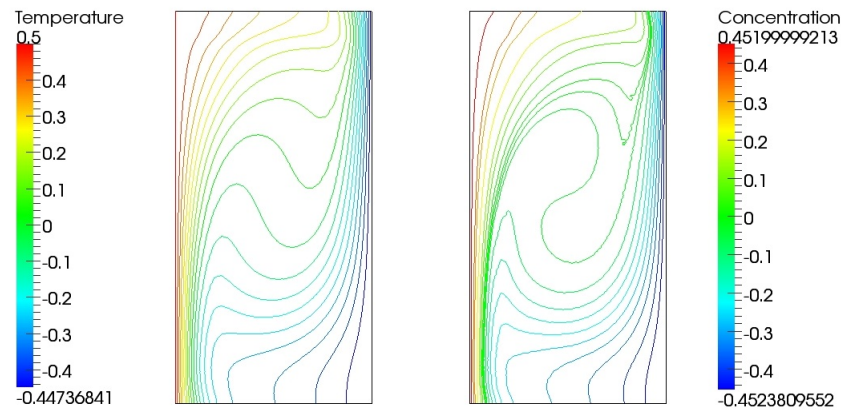


Figure 2: Results obtained with the stabilized finite element approach, for $Pr = 1, Le = 2, Ra = 10^5$ and $N = 0.8$

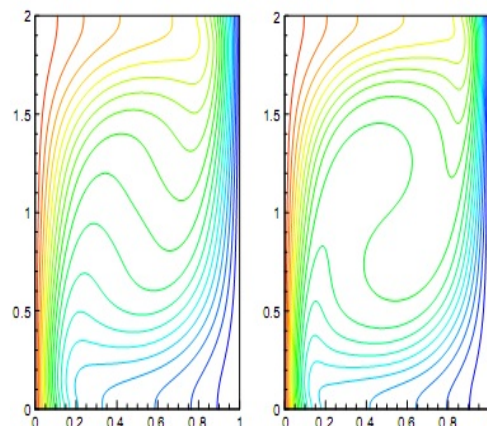


Figure 3: Results obtained by *Chen et al.*, for $Pr = 1, Le = 2, Ra = 10^5$ and $N = 0.8$

5 RESULTS

The influence of the nondimensional groups is analyzed here, by varying one of the groups while keeping the others constant and analyzing the behavior of the temperature and concentration. The mesh used varies in each analysis. This is made in order to capture the boundary layer structure properly, since changing some groups - such as the Rayleigh number - affects the characteristic velocity of the flow, and therefore the width of the boundary layer. Also, turbulent flow occurs in some cases, such that a more refined mesh is needed to capture large scale vortices. Using tetrahedra - which is a linear element - to discretize the whole domain also induces excessive refinement near the walls, since the fields there are known to be nonlinear. Ideally, a prism layer would be used to discretize the domain in the boundary layer, although this is not the case here.

5.1 Variation of the Lewis Number

The Lewis number influence in the solution was tested by setting $Le = 0.2$, $Le = 1$ and $Le = 5$, while keeping the other groups at constant value of $Pr = 1$, $Ra = 10^5$ and $N = 1$. A low value of Lewis number, which is the first case here, shown in figure 4, means a greater diffusivity rate of mass comparing to heat. In the initial timesteps, the front of concentration advances from left to right quickly than the temperature front. As the density increases with concentration (remember the negative sign of β_C) we have a region in the left where concentration has a higher value than the temperature, which implies an initial counterclockwise circulation in the cavity. The fluid then starts to carry the higher values of temperature and concentration passing by the bottom of the cavity to the right. At this moment, while in the bottom of the cavity, the higher diffusion of concentration acts pushing the intermediate values towards the top. The final profile is a balance between the temperature, which tries to push fluid clockwise, and concentration, which tries to push fluid counterclockwise. Concentration wins because of its better capability of spreading higher concentration values.

A not so interesting result is seen in the case with equal diffusivities, figure 5. As temperature and concentration behave in the same way, the forces made by the temperature and concentration cancel each other in both walls initially. As the fields diffuse exactly in the same way, these forces always balances equally, so that no flow exists through the domain and the fluid remains stationary. The final solution is just the diffusion of the fields through the domain.

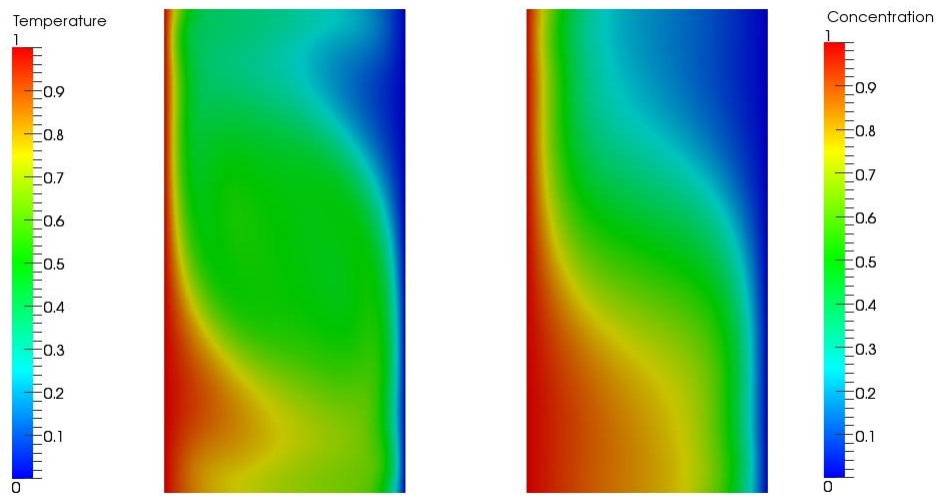


Figure 4: Steady-state solution, for $Pr = 1, Le = 0.2, Ra = 10^5$ and $N = 1$

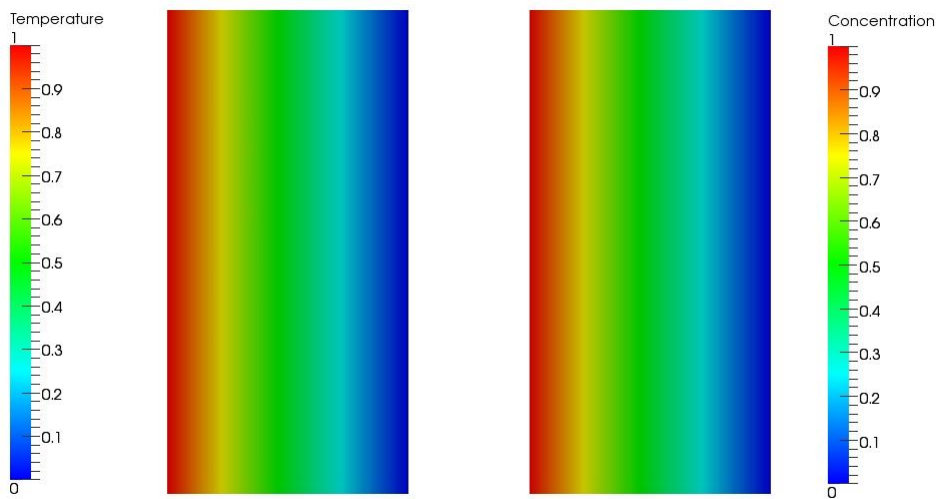


Figure 5: Steady-state solution, for $Pr = 1, Le = 1, Ra = 10^5$ and $N = 1$

5.2 Variation of the Buoyancy Ratio

Considering $N = 1.3$, as in the case of figure 6, means that density varies more with concentration as it does with temperature, by a factor of 1.3. This results in a similar physical behavior as seen in the first case of the section above. As the buoyancy ratio increases, the concentration stratification increases, as the force pushing the low concentration fluid up becomes greater. This can be seen in figure 7

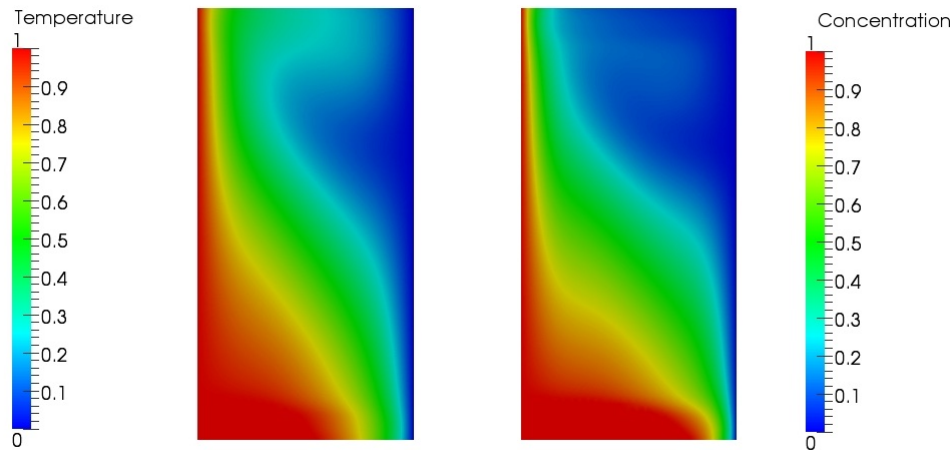


Figure 6: Steady-state solution, for $Pr = 1, Le = 2, Ra = 10^5$ and $N = 1.3$

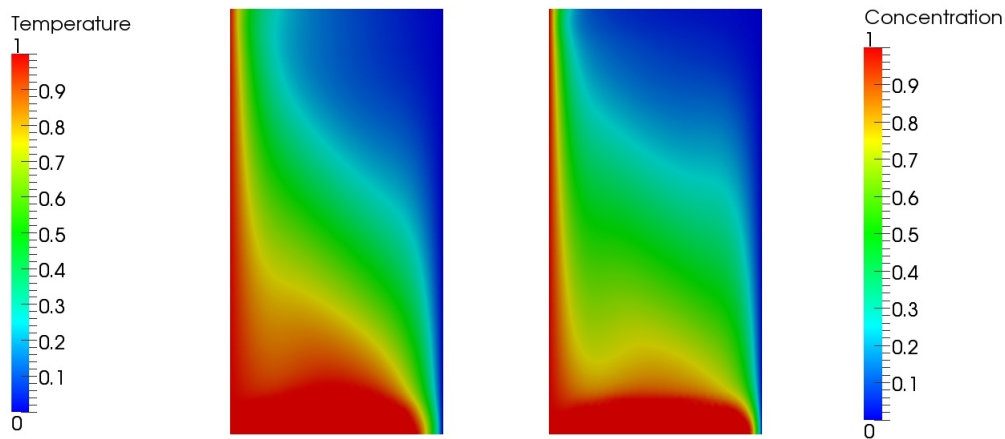


Figure 7: Steady-state solution, for $Pr = 1, Le = 2, Ra = 10^5$ and $N = 1.8$

5.3 Variation of the Rayleigh Number

Numerically and physically speaking, the increasing of the Rayleigh number makes the problem increasingly more challenging. For natural convection problems, a characteristic velocity can be taken to be $V = (gL\beta_{REF}\Delta T)^{1/2}$, such as increasing the Rayleigh number and keeping the diffusivities constant means increasing the characteristic velocity of the flow. This can trigger the flow to turbulent behavior. As the velocity increases, small perturbations in the mean fields can be amplified due to the nonlinear advection term in the Navier-Stokes equation. This may cause transition to turbulent flow, where a full spectra of scales is present, which means a difficult numerical problem.

Firstly, a $Ra = 10^6$ test was made, and the time scales were compared with the ones using the same values of N, Le and Pr , but with $Ra = 10^5$ (which was the case used in the validation section). Figures 8 and 10 show the evolution of the fields in the timesteps of $t = 0.011$ and $t = 0.033$ for $Ra = 10^5$, while figures 9 and 11 show the same results for the higher value of Rayleigh number. Note that the last case evolves much more quickly, and small perturbations can be seen in the fields. However, this value of Rayleigh is not enough to transition to turbulence. Figure 12 shows the contour of the steady-state solution for the $Ra = 10^6$ case.

In the $Ra = 10^7$ case, turbulent flow occurs. Figures 13,14,15 and 16 show the fields at various timesteps. One should note the presence of structures of various space scales. Also, one of the main characteristics of turbulence is observed: the diffusivities of the fields are increased. Temperature and concentration diffuses themselves much quickly, although steady-state behavior is not achieved. It is also to be noticed that, as velocity increases, the fields are much more similar to each other, because the other physical effects, as buoyancy and diffusion walk in the way of being negligible.

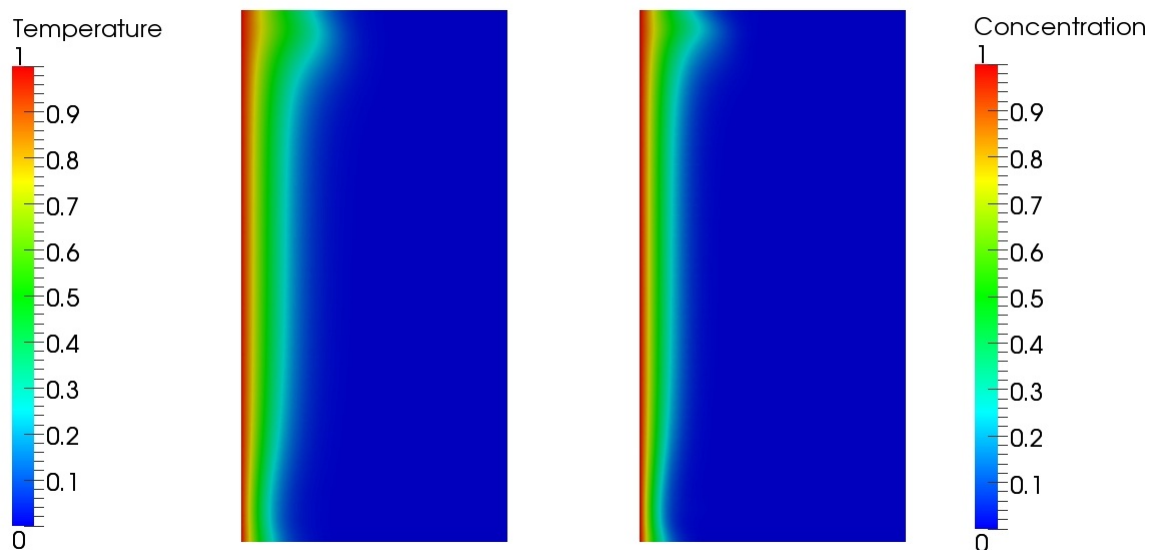


Figure 8: Results at $t = 0.011$, for $Pr = 1, Le = 2, Ra = 10^5$ and $N = 0.8$

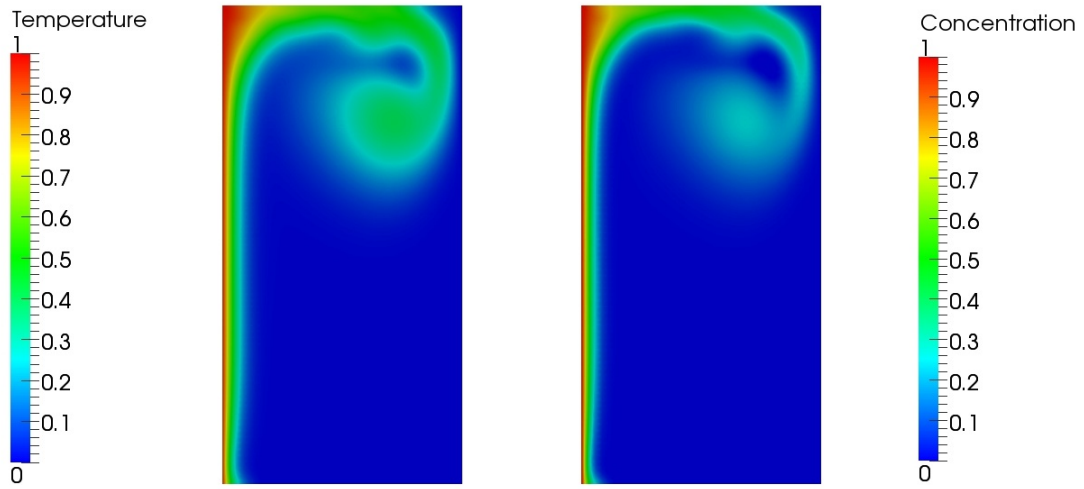


Figure 9: Results at $t = 0.011$, for $Pr = 1, Le = 2, Ra = 10^6$ and $N = 0.8$

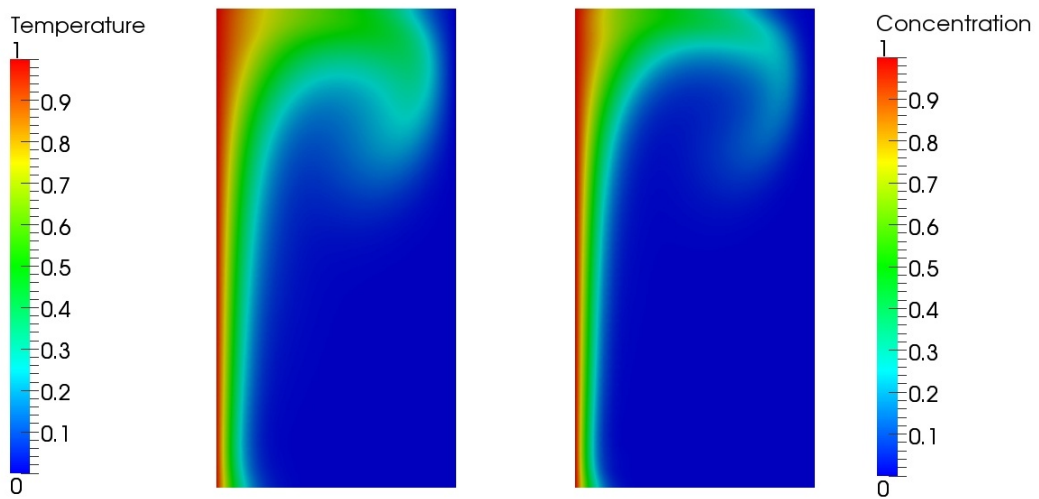


Figure 10: Results at $t = 0.026$, for $Pr = 1, Le = 2, Ra = 10^5$ and $N = 0.8$

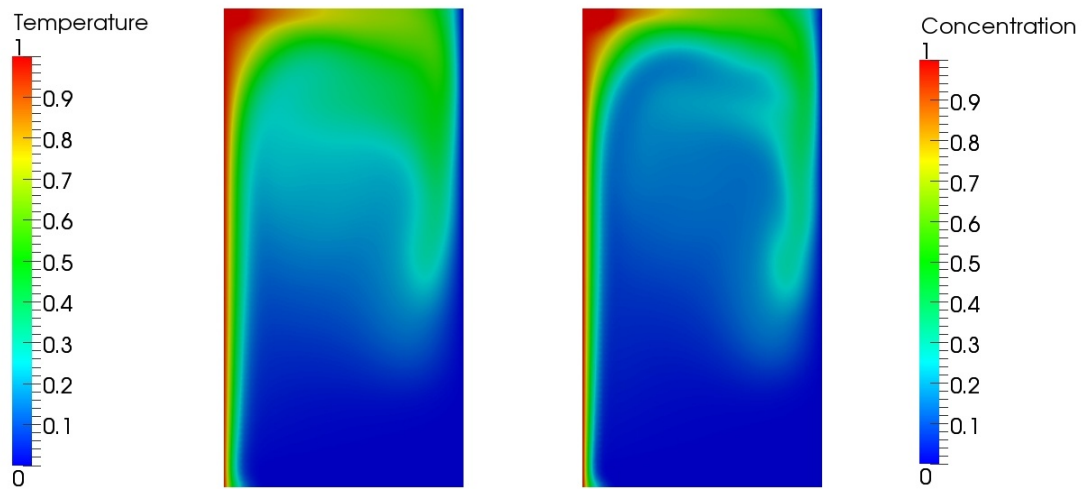


Figure 11: Results at $t = 0.026$, for $Pr = 1, Le = 2, Ra = 10^6$ and $N = 0.8$

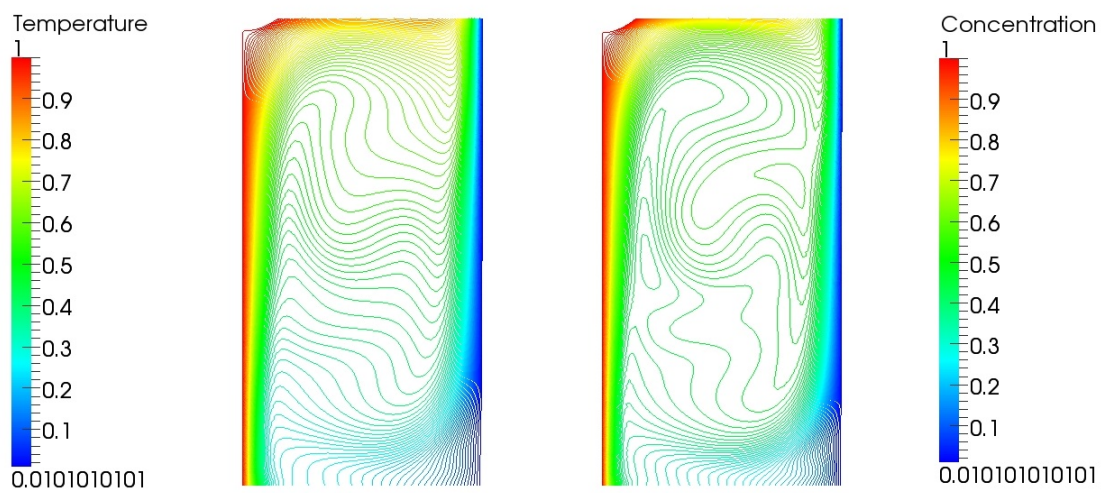


Figure 12: Contour of the steady-state, for $Pr = 1, Le = 2, Ra = 10^6$ and $N = 0.8$

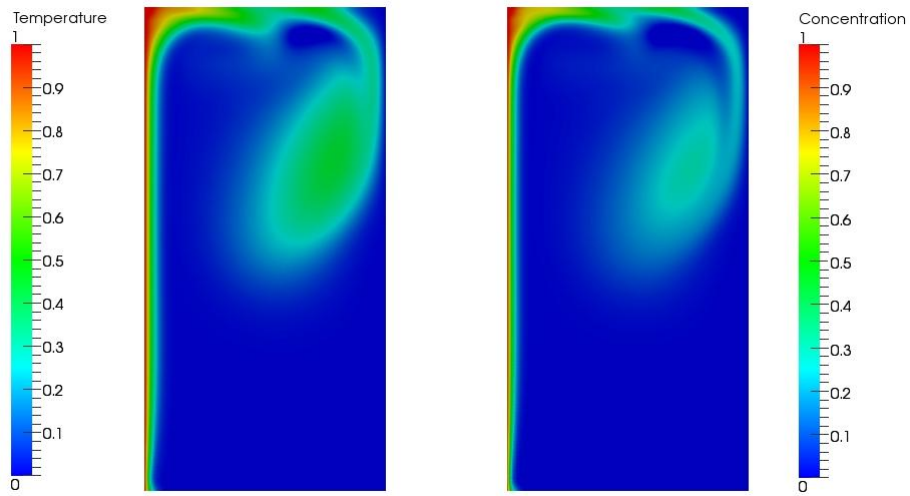


Figure 13: Results at $t = 0.002$, for $Pr = 1, Le = 2, Ra = 10^7$ and $N = 0.8$

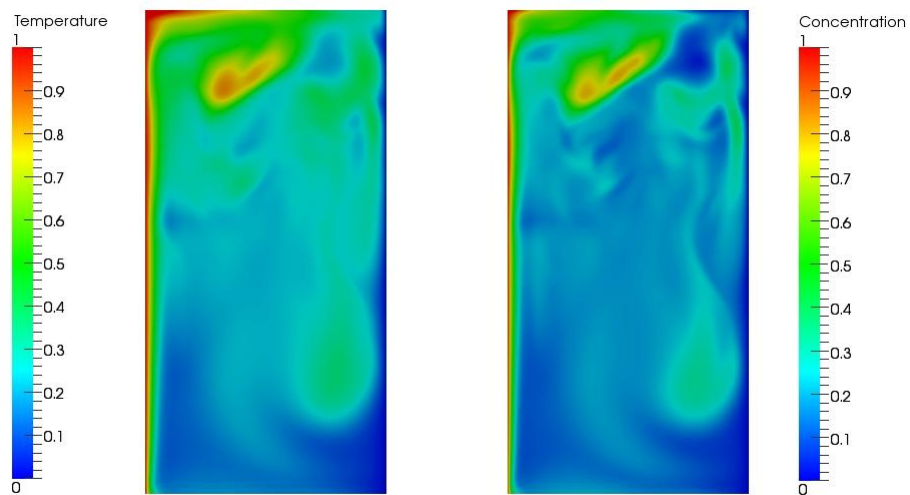


Figure 14: Results at $t = 0.004$, for $Pr = 1, Le = 2, Ra = 10^7$ and $N = 0.8$

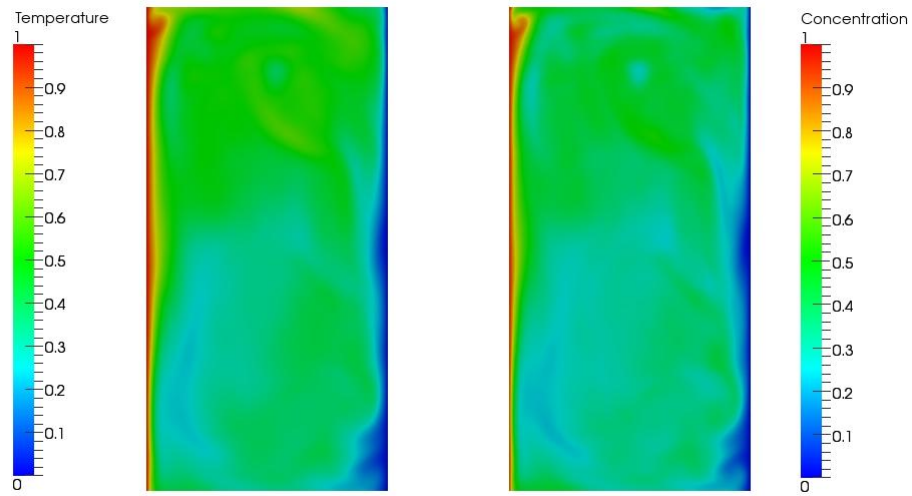


Figure 15: Results at $t = 0.011$, for $Pr = 1, Le = 2, Ra = 10^7$ and $N = 0.8$

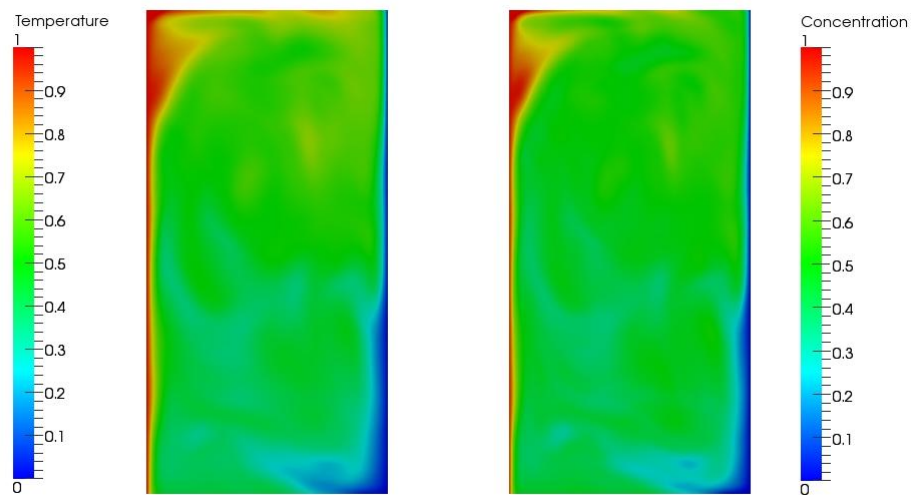


Figure 16: Results at $t = 0.026$, for $Pr = 1, Le = 2, Ra = 10^7$ and $N = 0.8$

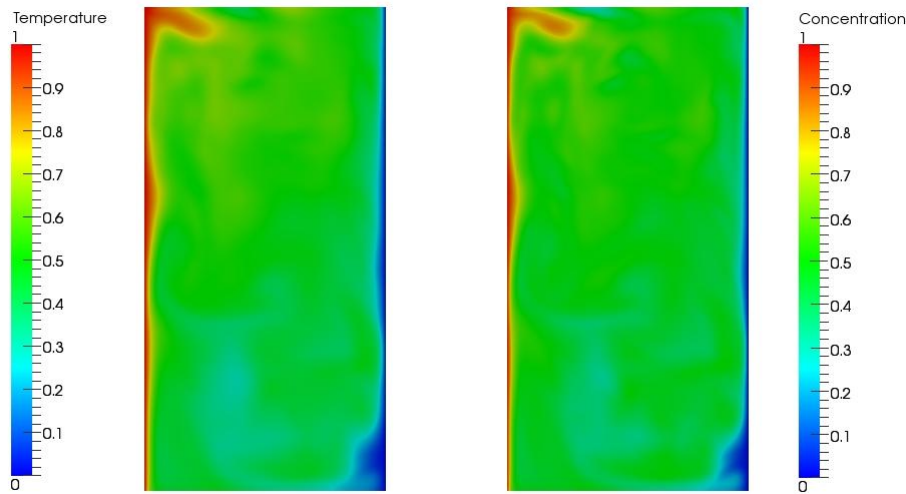


Figure 17: Results at $t = 0.050$, for $Pr = 1, Le = 2, Ra = 10^7$ and $N = 0.8$

6 CONCLUSION

This work used a stabilized finite element method for the solution of combined heat and mass transfer in a rectangular cavity. The values of the Lewis number, the buoyancy ratio and the Rayleigh number were modified while keeping the others constant to evaluate the influence of these groups in the temperature and concentration fields. The results were physically consistent, proving that this formulation is adequate for this complex multiphysics phenomena. It was shown that the groups tested have great influence on the steady state of the fields, and it was possible to see how do they affect the final distribution of the temperature and concentration. It was also shown that the frontier between the transient cases and the cases in which a steady-state is achieved lies between $Ra = 10^6$ and $Ra = 10^7$ for the given geometry. Future work may comprise a wider variation of the groups, the verification the influence of high order approximations for the density (such as in [Nithyadevi and Yang \(2009\)](#)) and the analysis of the influence of Dufour and Soret effects in this kind of problems.

7 ACKNOWLEDGMENTS

The authors thanks the *CAPES, CNPq* and *FAPERJ* funding agencies for providing the financial support to this research work. Computing resources were provided by *NACAD* - the High Performance Computing Center of *COPPE/UFRJ*

REFERENCES

- Brooks A.N. and Hughes T.J.R. Streamline upwind / petrov galerkin formulations for convection dominated flows with particular emphasis on the incompressible navier stokes equations. *Computer Methods in applied Mechanics and Engineering*, 32:199–259, 1982.
- Chamkha A.J. and Al-Naser H. Hydromagnetic double-diffusive convection in a rectangular enclosure with opposing temperature and concentration gradients. *International Journal of Heat and Mass Transfer*, 45:2465–2483, 2002.
- Chen S., Tolke J., and Krafczyk M. Numerical investigation of double-diffusive (natural) convection in vertical annulus with opposing temperature and concentration gradients. *International Journal of Heat and Fluid Flow*, 31:217–226, 2010.
- Cheng C.Y. Soret and dufour effects on natural convection heat and mass transfer from a vertical cone in a porous medium. *International Communications in Heat and Mass Transfer*, 36:1020–1024, 2009.
- Codina R. A discontinuity-capturing crosswind-dissipation for the finite element solution of the convection-diffusion equation. *Computer Methods in Applied Mechanics and Engineering*, 110:325–342, 1993.
- Elias R.N., Martins M.A.D., and Coutinho A.L.G.A. Inexact newton-type methods for the solution of steady incompressible viscoplastic flows with the supg / pspg finite element formulation. *Computer Methods Applied in Mechanics Engineering*, 195:3145–3167, 2006.
- Hughes T.J.R. *The Finite Element Method*, volume I. Dover Publications, 2003.
- Kamakura K. and Ozoe H. Three-dimensional analyses of double diffusive convection in a two-layer system at high rayleigh number. *International Journal of Thermal Sciences*, 41:1045–1053, 2002.
- Kim C.N. and Rani H.P. A numerical study of the dufour and soret effects on unsteady natural convection flow past an isothermal vertical cylinder. *Korean Journal of Chemical Engineering*, 26:946–954, 2009.
- Nithyadevi N. and Yang R.J. Double diffusive natural convection in a partially heated enclosure with soret and dufour effects. *International Journal of Heat and Fluid Flow*, 30:902–910, 2009.
- Sezai I. and Mohamad A.A. Double diffusive convection in a cubic enclosure with opposing temperature and concentration gradients. *Physics of Fluids*, 12:2210–2223, 2000.
- Sripada R.K.L. and Angirasa D. Simultaneous heat and mass transfer by natural convection-above upward facing horizontal surfaces. *International Journal of Non-Linear Mechanics*, 36:1019–1029, 2001.
- Tezduyar T.E. Stabilized finite element formulations for incompressible flow computations. *ADVANCES IN APPLIED MECHANICS*, 28:1–44, 1992.
- Yahiaoui M.A., Bahloul A., Vasseur P., and Robillard L. Natural convection of a binary mixture in a vertical closed annulus. *Chemical Engineering Communications*, 194:924–937, 2007.